

## Electron-electron interaction and intersubband absorption coefficient in a GaAs/Al<sub>x</sub>Ga<sub>1-x</sub>As quantum well

Paul von Allmen\*

*IBM Research Division, Zurich Research Laboratory, 8803 Rüschlikon, Switzerland*

(Received 26 December 1991)

The full random-phase approximation (RPA) spectral function is calculated for an electron gas confined in a modulation-doped GaAs/Al<sub>x</sub>Ga<sub>1-x</sub>As quantum well. In the first subband we observe the typical structure of the two-dimensional plasmaron. The renormalization of the chemical potential is smaller than that of the edge of the density of states. In the second subband the single-state broadening and the band renormalization are found to be smaller than in the first subband. When the depolarization effect is neglected, the intersubband absorption line is narrower than the inhomogeneous broadening due to the different effective masses in the two subbands for the noninteracting electron system. This result is explained by the two-dimensional plasmaron structure in the first subband. The theoretical peak is narrower than the experimental one. If in the spectral function the self-energy is taken at the energy of the noninteracting electron, the corresponding absorption line is broader than the experimental one. If the depolarization effect is included, the approximate linewidth is found to be narrower and the full RPA linewidth broader than the experimental one.

### I. INTRODUCTION

Intersubband transitions in a confined electron gas have been intensively studied in the past decades. Experimentally, they have been observed by absorption spectroscopy in Si inversion layers (see Ref. 1 and references therein) and in GaAs/Al<sub>x</sub>Ga<sub>1-x</sub>As quantum wells.<sup>3,4</sup> They have also been studied with Raman-scattering experiments.<sup>5</sup> There are two main reasons for the large interest in these transitions. First there is a technological interest for their potential application as detectors and eventually as emitters in a spectral range for which only few tools are available.<sup>2</sup> Second, they offer the opportunity to study a relatively simple system with a confined electron gas and thereby provide us with a good benchmark for testing the validity of several approximations that are widely used when dealing with electron-electron interactions in a many-body system.

Several authors have calculated the position of the intersubband absorption peak, including the effect of the electron-electron interaction.<sup>6-8</sup> Good qualitative agreement was obtained. Concerning the line shape, attempts were made to calculate the absorption line by approximating the single-state broadening function by a Lorentzian.<sup>4</sup> In this picture, the simplest approximation for the broadening parameter (half-width at half-height of the Lorentzian) is the imaginary part of the self-energy calculated with the random-phase approximation (RPA) and taken at the noninteracting electron energy. The theoretical value extrapolated from the results reported in the literature<sup>9</sup> is larger than the value obtained by fitting the experimental to the theoretical spectra. On the other hand, the screening of the photon line by the polarization of the confined electron gas (depolarization effect) was shown to make the line narrower.<sup>10</sup> But, at low temperature, the effect is only about 20% and does not remove the discrepancy between experiment and theory.

In this work, the full RPA spectral function is used to describe the broadening of the single state when the intersubband absorption coefficient is calculated. Without any fitting procedure, a theoretical absorption line is obtained that is narrower than the experimental one. It will be shown that the origin of this result is in the structure of the two-dimensional plasmaron excitation described elsewhere.<sup>11</sup>

### II. THEORY

The absorption coefficient  $\alpha$  is obtained from the real part of the electrical conductivity that is related by a Kubo formula to the retarded form of the current-current correlation function  $\Pi(\omega)$ ,<sup>12</sup>

$$\alpha(\omega) = \frac{1}{nc\epsilon_0\omega V} \text{Im}[\Pi(\omega)] . \quad (1)$$

The refractive index is  $n$ , the velocity of the light in the vacuum is  $c$ , the vacuum dielectrical permittivity is  $\epsilon_0$ , and the volume of the crystal is  $V$ .

For the evaluation of  $\Pi(\omega)$ , we neglect the diagrams that describe the final-state interactions (excitonic effect). This effect was shown to be small for intersubband transitions.<sup>6</sup> In a first step, we also neglect the screening by the polarization of the confined electron gas (depolarization effect).

The Matsubara form of the current-current correlation function is then given by the following expression:

$$\Pi(i\omega_m) = |p_z^{1,2}|^2 \sum_k \frac{1}{\beta} \sum_{ik_n} \mathcal{G}_{22}(k, ik_n + i\omega_m) \mathcal{G}_{11}(k, ik_n) . \quad (2)$$

The Fermi and Bose imaginary frequencies are  $ik_n$  and  $i\omega_m$ , respectively. The momentum matrix element be-

tween the two levels for light polarized in the  $z$  direction (perpendicular to the layers) is  $p_z^{1,2}$ . It is taken to be independent of the momentum  $k$ , which is a good assumption for the conduction subbands considered in the following. The temperature  $T$  appears in  $\beta=1/k_B T$ , where  $k_B$  is the Boltzmann constant. The dressed one-particle Green's function in band  $j$  is  $\mathcal{G}_{jj}$ . We note that in expression (2) we keep only the main contribution when band 2 is at a higher energy than band 1.

After frequency summation and using the spectral representation for the Green's function, we obtain the following expression for the absorption coefficient:

$$\alpha(\omega) = \frac{|p_z^{1,2}|^2}{nc\epsilon_0\omega} \frac{1}{(2\pi)^2} \times \int d^3k \int dE \frac{A_2(k, E+\omega)}{2\pi} \frac{A_1(k, E)}{2\pi} \times [n_F(E) - n_F(E+\omega)], \quad (3)$$

where  $n_F$  is the Fermi distribution function.

We obtain the spectral functions  $A_j$  ( $j=1,2$ ) by solv-

ing the Dyson equation for a two-band system.<sup>6</sup> In this procedure, we neglect the vertices for the electron-electron scattering in which an electron scatters from one band to the other.<sup>6</sup> The justification for this approximation is that the corresponding matrix elements of the Coulomb potential do not diverge at  $q=0$ , whereas they do diverge if the electrons stay in the same subband during the scattering. The polarization in the second band is also neglected.<sup>6</sup> This assumption is acceptable if the second band is almost empty, which is the case in the example presented below.

The spectral functions can then be written as follows:

$$A_j(k, E) = \frac{-2\mathcal{S}_{jj,I}(k, E)}{[E - \xi_j(k) - \mathcal{S}_{jj,R}(k, E)]^2 + [\mathcal{S}_{jj,I}(k, E)]^2}. \quad (4)$$

Measured from the chemical potential  $\mu$ , the kinetic energy of the noninteracting electron, in band  $j$ , with effective mass  $m_j$ , is  $\xi_j(k) = E_{0j} + (\hbar^2 k^2 / 2m_j) - \mu$ . The real ( $\mathcal{S}_{jj,R}$ ) and imaginary ( $\mathcal{S}_{jj,I}$ ) parts of the self-energy are evaluated in the RPA,

$$\mathcal{S}_{11}(k, E) = -\frac{1}{(2\pi)^2} \int d^2q v_{1111}(q) \left[ n_F[\xi_1(\mathbf{k}+\mathbf{q})] + \int \frac{dE'}{2\pi} C_1(q, E') \frac{n_F[\xi_1(\mathbf{k}+\mathbf{q})] + n_B(E')}{E' - \xi_1(\mathbf{k}+\mathbf{q}) + E + i\delta} \right], \quad (5)$$

$$\mathcal{S}_{22}(k, E) = -\frac{1}{(2\pi)^2} \int d^2q \left[ v_{2222}(q) n_F[\xi_2(\mathbf{k}+\mathbf{q})] + \frac{v_{1122}^2(q)}{v_{1111}(q)} \int \frac{dE'}{2\pi} C_1(q, E') \frac{n_F[\xi_2(\mathbf{k}+\mathbf{q})] + n_B(E')}{E' - \xi_2(\mathbf{k}+\mathbf{q}) + E + i\delta} \right], \quad (6)$$

where  $C_1(q, E) = -2 \text{Im}[1 - v_{1111}(q)P_{11}^{(1)}(q, E)]^{-1}$  is the RPA charge-density excitation function in band 1, and  $P_{11}^{(1)}(q, E)$  is the single-bubble polarization function in band 1 whose analytical expression at  $T=0$  K is well known.<sup>13</sup> The Bose distribution function is  $n_B$ .

The unscreened Coulomb potential, in mks units, is given by the usual expression,<sup>6</sup>

$$v_{ij'jj'}(q) = \frac{1}{d^2} \sum_{n, n'=1}^N \int_0^d dz_1 \int_0^d dz_2 v(q, z_1 - z_2) \times \phi_n^{(j')*}(z_1) \phi_n^{(j)}(z_1) \times \phi_{n'}^{(i')*}(z_2) \phi_{n'}^{(i)}(z_2), \quad (7)$$

where

$$v(q, z) = \int d^2r e^{iq \cdot r} \frac{e^2}{4\pi\epsilon\sqrt{r^2 + z^2}} = \frac{e^2}{2\epsilon q} e^{-q|z|}. \quad (8)$$

The envelope functions for subband number  $j$  are given by  $\phi_n^{(j)}(z)$  with  $n=1, \dots, N$ , where  $N$  is the number of bands taken into account for the subband calculation. The period of the superlattice is  $d$  and the background static dielectric constant  $\epsilon$ . We assume that the envelope functions  $\phi_n^{(j)}$  describing the noninteracting electron states in the quantum well are independent of the momentum  $k$ . This is a good approximation for conduction subbands, which is the case we consider below.

The transitions described by (2) are coupled by scattering events in which one electron jumps from band 1 to band 2 while another jumps from band 2 to band 1.<sup>6</sup> The corresponding matrix element of the Coulomb potential is  $v_{1221}(0)$  and the current-current correlation function is

$$\Pi^{(S)}(\omega) = |p_z^{1,2}|^2 \frac{\pi^{(0)}(\omega)}{1 - v_{1221}(0)\pi^{(0)}(\omega)}, \quad (9)$$

where  $\pi^{(0)}(i\omega_m) = \Pi(i\omega_m) / |p_z^{1,2}|^2$ . The absorption coefficient is given by (1) with  $\Pi^{(S)}$  replacing  $\Pi$ . This screening mechanism was first described in Ref. 14 and leads to the well-known depolarization shift. In the next section we shall compare the line shapes with and without depolarization effect.

The subband energy dispersion is obtained by solving the effective-mass  $\mathbf{k} \cdot \mathbf{p}$  equation self-consistently with the Poisson equation.<sup>4</sup> For the  $\mathbf{k} \cdot \mathbf{p}$  Hamiltonian, we include 14 bands ( $\Gamma_6^c$ ,  $\Gamma_7^v$ ,  $\Gamma_8^v$ ,  $\Gamma_7^c$ , and  $\Gamma_8^c$ ) explicitly, which is necessary if the nonparabolicity of the bulk material and hence the effective mass of the subbands have to be known with precision.<sup>15</sup> For the calculation of the self-energy, the subbands are assumed to be parabolic. This is a good approximation for the charge density used below for which the electron population at low temperature is confined to small values of the momentum.

In our calculation, the chemical potential is given and

the charge density is evaluated with the following expression:

$$n_S = \frac{2}{(2\pi)^2} \int d^2k \int \frac{dE}{2\pi} \sum_{j=1}^2 A_j(k, E) n_F(E). \quad (10)$$

As already discussed elsewhere,<sup>11</sup> a different procedure is often used in the literature. The charge density is given and the chemical potential is evaluated in the lowest-order approximation,<sup>16</sup>

$$\mu = \frac{\hbar^2 k_F^2}{2m_1} + \mathcal{S}_{11,R}^{(0)}(k_F, 0), \quad (11)$$

where  $k_F = \sqrt{2\pi n_S}$  is the Fermi momentum. The superscript (0) in  $\mathcal{S}_{11,R}^{(0)}$  indicates that the self-energy is evaluated using the chemical potential of the noninteracting electron gas  $\mu^{(0)} = (\hbar^2 k_F^2)/2m_1$ . In expression (11), it is assumed that only band 1 is populated, which is the case for the example treated below.

In Ref. 11 we have already discussed the lowest-order approximation in connection with the band renormalization. Here we shall study its impact on the intersubband absorption line. We shall compare our result with the line shape obtained by using an approximate spectral function  $A_j^{(0)}$  in which the self-energy function is taken as  $\mathcal{S}_{jj}^{(0)}(k) = \mathcal{S}_{jj}^{(0)}[(k, \hbar^2(k^2 - k_F^2)/2m_j)]$ .

### III. RESULTS

The electron gas is confined in a 80-Å-wide GaAs well surrounded by two 250-Å-wide Al<sub>0.35</sub>GaAs barriers, whose 50-Å-wide central parts are *n* doped with a Si concentration of  $N_d = 1.6 \times 10^{18} \text{ cm}^{-3}$ . Solving the effective-mass *k*·*p* equation at *T*=0 K self-consistently with the Poisson equation gives two conduction subbands whose energy separation at *k*=0 is  $\Delta E = 123 \text{ meV}$ . The corresponding effective masses are  $m_1 = 0.0722m_0$  and  $m_2 = 0.0874m_0$ , where  $m_0$  is the mass of the free electron.

Using these parameters, we calculate the spectral function at *T*=0 K for the two subbands with a chemical potential  $\mu = 19 \text{ meV}$ , counted from the edge of the first subband. The relative background dielectric constant is  $\epsilon_r = 12.5$ .

Figure 1 displays the resulting curves for two values of the momentum:  $k=0$  and  $k=k_F=0.0231 \text{ \AA}^{-1}$ . At  $k=0$ , the spectral function for the first subband has two peaks with approximately the same spectral weight. At  $k=k_F$ , most of the spectral weight is in the  $\delta$  function situated at the Fermi surface ( $E=0$ ). This behavior is identical to that found for a pure two-dimensional (2D) electron gas and has been described in detail in Ref. 11. The low-energy peak at  $k=0$  is ascribed to the plasmaron excitation that was identified for a three-dimensional electron gas in Ref. 17.

The spectral function for the second subband also shows two peaks with about 85% of the spectral weight in the low-energy peak. This peak is a  $\delta$  function at  $k=0$ , and an approximately 1-meV-wide peak at half height at  $k=k_F$ .

Figure 1 also displays the approximate spectral func-

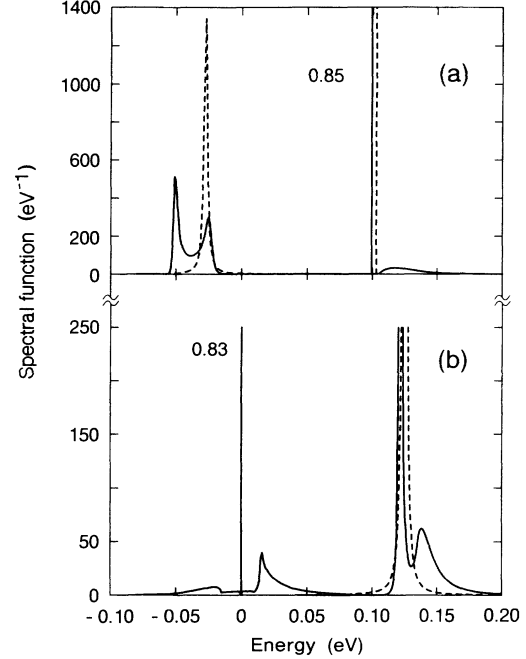


FIG. 1. Spectral function at *T*=0 K for the first and second subband in a modulation-doped quantum well for a charge density  $n_S = 8.1 \times 10^{11} \text{ cm}^{-2}$ . (a)  $k=0$  and (b)  $k=k_F=0.023 \text{ \AA}^{-1}$ ; solid line: full RPA calculation; dashed line: lowest-order approximation. The numbers next to the  $\delta$  functions indicate their spectral weight for the full RPA calculation.

tion  $A_j^{(0)}$ . At  $k=0$ , for the first subband it is a Lorentzian, narrower than the two peaks of  $A_1$  and centered at about the same position as the high-energy peak of  $A_1$ . For the second subband it is a  $\delta$  function positioned a little above the  $\delta$  function in  $A_2$ . At  $k=k_F$ ,  $A_1^{(0)}$  is a  $\delta$  function centered at  $E=0$  and  $A_2^{(0)}$  is a Lorentzian, a little broader than and situated slightly higher than the first peak in  $A_2$ .

To explain the shape of the intersubband absorption line, we display the dispersion of the quasiparticle (QP) energy and width in Fig. 2.

The QP energy for band number  $j$  ( $E_j^{(\text{QP})}$ ) is given by the solution of the following equation:

$$E_j^{(\text{QP})} - \xi_j(k) - \mathcal{S}_{jj,R}(k, E_j^{(\text{QP})}) = 0. \quad (12)$$

For the first subband, at  $k=0$ , there are three solutions to (12). The low-energy solution is associated with the low-energy peak in Fig. 1 and the two other solutions are associated with the second peak in the spectral function. The dispersion of the position of the first peak is nonparabolic: it presents a high (low) curvature for low (high) momenta. The dispersion for the second peak is parabolic with a curvature close to that of the high-momentum section for the first peak. Around  $k=0.015 \text{ \AA}^{-1}$ , the two peaks of the spectral function merge.

For the second subband, there is only one solution to (12) giving the low-energy peak of the spectral function (see Fig. 1). The dispersion is parabolic with an effective

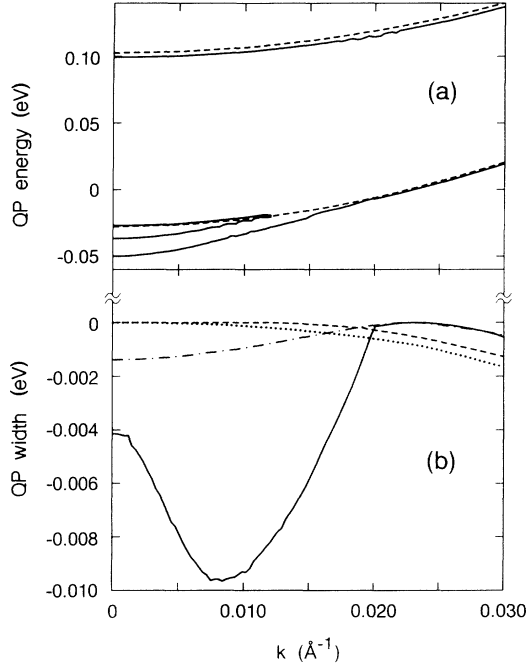


FIG. 2. Quasiparticle energy and width dispersion at  $T=0$  K for the first and second subband in a modulation-doped quantum well for a charge density  $n_S=8.1 \times 10^{11} \text{ cm}^{-2}$ . (a) Solid line: full RPA calculation; dashed line: lowest-order approximation. (b) Solid line: first subband, full RPA calculation; dashed line: second subband, full RPA calculation; dashed dotted line: first subband, lowest-order approximation; dotted line: second subband, lowest-order approximation.

mass  $m_2^*=0.091m_0$ , very close to that of the noninteracting electron. The origin of the second peak in the spectral function is a resonance in the imaginary part of the self-energy that is associated with an enhancement in the electron-plasmon scattering cross section.

The width of the QP ( $\Gamma_j^{(\text{QP})}$ ) is given by the imaginary part of the self-energy taken at the energy of the QP. For the first subband, we give the dispersion of the width for the low-energy peak. It is small in a region near  $k=0$ , then increases, reaches a maximum and decreases to reach zero at  $k=k_F$ , as expected from the Fermi-liquid theory.<sup>18</sup> For the second subband, the width, starting from zero, steadily increases with increasing  $k$ . We note that the shape of the QP energy and width dispersion for the first subband is identical to that for a purely 2D electron gas.<sup>11</sup>

Figure 2 also displays the QP energy and width dispersion in the lowest-order approximation. The QP energy is given by

$$\bar{E}_j^{(\text{QP})}(k) = \xi_j(k) + \mathcal{S}_{jj,R}^{(0)} \left[ k, \frac{k^2 - k_F^2}{2m_j} \right] \quad (13)$$

and the width by

$$\bar{\Gamma}_j^{(\text{QP})}(k) = \mathcal{S}_{jj,I}^{(0)} \left[ k, \frac{k^2 - k_F^2}{2m_j} \right]. \quad (14)$$

The energy dispersion is parabolic for the two subbands. For the first subband it is very close to the dispersion of the high-energy peak in  $A_1$ . For the second subband,  $\bar{E}_2^{(\text{QP})}$  is a little larger than  $E_2^{(\text{QP})}$  and the dispersion is nearly parallel.

The width dispersion for the first subband is identical to what can be found in the literature:<sup>9</sup> it decreases with increasing  $k$ , reaches zero at  $k=k_F$ , and then increases again. For the second subband  $\bar{\Gamma}_2^{(\text{QP})}$  is slightly larger than  $\Gamma_2^{(\text{QP})}$ , but the shape of the dispersion is identical.

The charge density obtained from (10) is  $n_S=8.1 \times 10^{11} \text{ cm}^{-2}$  and the corresponding renormalization of the chemical potential is  $\Delta^{(\mu)} = \mu - (\hbar^2 \pi n_S / m_1) = -8.5 \text{ meV}$ . The shift of the edges of the density of states (DOS) is given by the QP energy at  $k=0$ .<sup>11</sup> The values for subbands 1 and 2 are  $\Delta_1^{(\text{DOS})} = -50 \text{ meV}$  and  $\Delta_2^{(\text{DOS})} = -24 \text{ meV}$ , respectively. As reported in Ref. 19, the renormalization for the second subband represents a sizable fraction of that for the first subband.<sup>20</sup> Also, as already discussed in Ref. 11, the shift of the chemical potential is smaller than that of the edge of the DOS.

The normalized absorption coefficient given by (3) is presented in Fig. 3(a). The complicated structure of the QP energy and width dispersion is reflected in the absorption coefficient.

We observe a broad absorption band ranging from

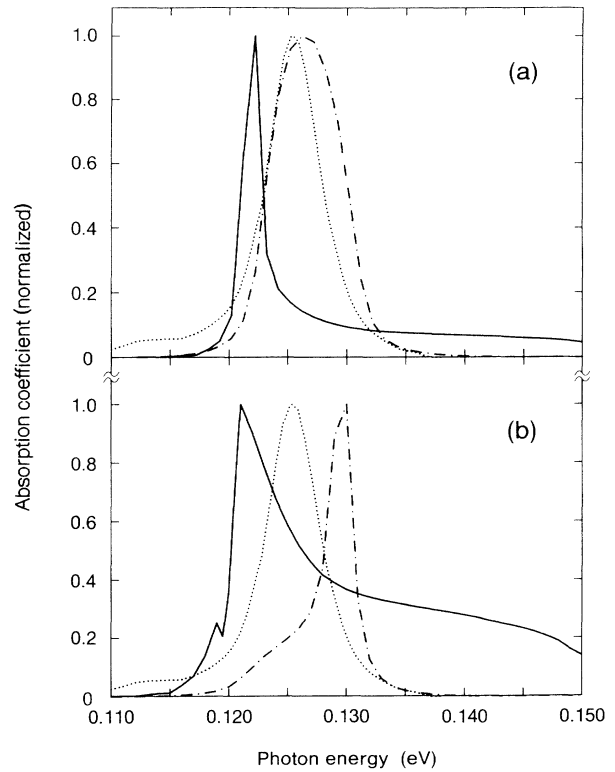


FIG. 3. Intersubband absorption coefficient at  $T=0$  K for a modulation-doped quantum well (a) without and (b) with depolarization effect. Solid line: with the full RPA spectra function; dashed-dotted line: with the RPA spectral function in the lowest-order approximation; dotted line: experimental spectrum from Ref. 4.

about 120 to 150 meV. It corresponds to the transitions starting from the high-curvature section in the first QP subband. The absorption occurs in a broad energy range because the curvatures of the two QP subbands are quite different in the corresponding low-momentum sections.

The sharp peak at about 120 meV stems from the transitions originating in the low-curvature section in the first QP subband. Its full width at half-height is about  $\Delta = 1.5$  meV. This is narrower than the width  $\Gamma^{(m)}$  deduced from the difference between the effective masses in the two subbands for the noninteracting electron system<sup>4,21</sup> (inhomogeneous broadening),

$$\Gamma^{(m)} = \frac{\hbar^2 k_F^2}{2} \left[ \frac{1}{m_1} - \frac{1}{m_2} \right] = 4.7 \text{ meV} . \quad (15)$$

The reason is that the momentum range in which the transitions contributing to the sharp peak occur is small:  $[k_i, k_F]$  with  $k_i = 0.02 \text{ \AA}^{-1}$ . The corresponding inhomogeneous broadening is

$$\Gamma^{(m)*} = \Delta E^{(\text{QP})}(k_i) - \Delta E^{(\text{QP})}(k_F) \simeq 0.9 \text{ meV} \quad (16)$$

with  $\Delta E^{(\text{QP})}(k) = E_2^{(\text{QP})}(k) - E_1^{(\text{QP})}(k)$ .

The transitions in the range  $[k_i, k_F]$  give a large contribution to the absorption spectra because the QP subbands are almost parallel in this region and because the corresponding QP width in the first subband is small.

Concerning the single-state broadening, Fig. 2(b) shows that the second subband gives the main contribution in this momentum range:  $\Gamma_2^{(\text{QP})} \simeq 0.4$  meV and  $\Gamma_1^{(\text{QP})} \simeq 0.06$  meV. To conclude, we see that the main contribution to the width of the sharp peak is the inhomogeneous broadening.

The position of the sharp peak is approximately equal to the energy separation between the QP subbands at the Fermi momentum [see Fig. 2(a)]. One could intuitively expect that the absorption peak is positioned at the average value of the transition energies at  $k=0$  and  $k=k_F$ :  $[\Delta E^{(\text{QP})}(0) + \Delta E^{(\text{QP})}(k_F)]/2$ . We see that this is not the case owing to the plasmaron-related structure in the first QP subband.

The slow decrease on the high-energy side of the sharp peak is attributed to the contribution of the high-energy peak in the spectral function of the first subband.

Figure 3(a) also displays the intersubband absorption line obtained by using the approximate spectral function  $A_j^{(0)}(k, E)$ . The peak is much broader and situated at a higher energy than that obtained with the full calculation. Its full width at half-height is  $\bar{\Delta} = 7.2$  meV. The main contribution comes from the inhomogeneous broadening,

$$\bar{\Gamma}^{(m)*} = \bar{\Delta E}^{(\text{QP})}(0) - \bar{\Delta E}^{(\text{QP})}(k_F) \simeq 6.6 \text{ meV} . \quad (17)$$

Its position is close to  $[\bar{\Delta E}^{(\text{QP})}(0) + \bar{\Delta E}^{(\text{QP})}(k_F)]/2$ ,

which is the value one intuitively expected.

Figure 3(a) also displays the experimental absorption line for the structure considered here.<sup>4</sup> Its full width at half-height is  $\Delta^{(\text{exp})} = 5.3$  meV. It is important to note that only the full RPA calculation gives a smaller linewidth, leaving room for broadening mechanisms other than electron-electron interaction.

Figure 3(b) displays the absorption spectra obtained by including the depolarization effect. As already shown in Ref. 10 the line shape is strongly modified. The absorption line evaluated in the lowest-order approximation is almost three times narrower than the peak without depolarization effect ( $\bar{\Delta}^{(S)} = 2.5$  meV). It is narrower than the experimental peak. Qualitatively the effect is the same as in Ref. 10, but it is much larger. The peak is at a  $\bar{\delta} = 6$  meV higher energy than without depolarization effect. This depolarization shift is reasonably close to the experimental value of  $\delta^{(\text{exp})} = 9$  meV.<sup>22</sup>

The absorption line evaluated by using the full RPA spectral function is almost four times broader than the peak without depolarization effect ( $\Delta^{(S)} = 5.7$  meV). It is broader than the experimental peak. This behavior can be intuitively understood from the coupling of the sharp peak obtained without depolarization effect with the broad absorption band associated with the high-curvature region in the first QP subband. The peak is at a  $\bar{\delta} = 1.5$  meV higher energy than without depolarization effect. This is much smaller than the experimental value.

The discrepancy between the, in principle, more accurate full RPA evaluation and the experimental data shows that some of the effects that have been neglected are important when the depolarization effect is included. I believe that the excitonic effect could be important for the line shape because it includes additional Coulomb lines in the calculation of the current-current correlation function, in a similar way as the depolarization effect does.

#### IV. CONCLUSION

We showed that the full and the approximate RPA spectral functions lead to an absorption line that is narrower and broader, respectively, than the experimental spectra if the depolarization effect is neglected. If we include the depolarization effect the approximate absorption line is narrower than the experimental one whereas the full RPA line is broader. This implies that effects that were neglected in this work, such as the excitonic effect, have to be considered in future calculations.

#### ACKNOWLEDGMENTS

I am indebted to A. Baratoff and M. Lax for fruitful discussions.

\*Present address: Beckman Institute, University of Illinois at Urbana-Champaign, Urbana, IL 61801. Electronic address: vonAllmen@gate.spg.edu

<sup>1</sup>Soe-Mie Nee, U. Claessen, and F. Koch, Phys. Rev. B **29**, 3449

(1984).

<sup>2</sup>B. F. Levine, K. K. Choi, C. G. Bethea, J. Walker, and R. J. Malik, Appl. Phys. Lett. **50**, 1092 (1987).

<sup>3</sup>L. C. West, and S. J. Eglash, Appl. Phys. Lett. **46**, 1156 (1985).

- <sup>4</sup>P. von Allmen, M. Berz, G. Petrocelli, F.-K. Reinhart, and G. Harbeke, *Semicond. Sci. Technol.* **3**, 1211 (1988); P. von Allmen, M. Berz, F.-K. Reinhart, and G. Harbeke, *Superlatt. Microstruct.* **5**, 259 (1989).
- <sup>5</sup>A. Pinczuk, J. Shah, A. C. Gossard, and W. Wiegmann, *Phys. Rev. Lett.* **46**, 1241 (1981).
- <sup>6</sup>B. Vinter, *Phys. Rev. B* **15**, 3947 (1977).
- <sup>7</sup>T. Ando and S. Mori, *J. Phys. Soc. Jpn.* **47**, 1518 (1979).
- <sup>8</sup>D. H. Ehlers, *Phys. Rev. B* **38**, 9706 (1988).
- <sup>9</sup>H. Haug and D. B. Tran Thoai, *Phys. Status Solidi B* **98**, 581 (1980).
- <sup>10</sup>M. Zaluzny, *Phys. Rev. B* **43**, 4511 (1991).
- <sup>11</sup>P. von Allmen, *Phys. Rev. B* (to be published).
- <sup>12</sup>See, e.g., G. D. Mahan, *Many-Particle Physics* (Plenum, New York, 1986).
- <sup>13</sup>F. Stern, *Phys. Rev. Lett.* **18**, 546 (1967).
- <sup>14</sup>S. J. Allen, Jr., D. C. Tsui, and B. Vinter, *Solid State Commun.* **20**, 425 (1976).
- <sup>15</sup>U. Rössler, *Solid State Commun.* **49**, 943 (1984).
- <sup>16</sup>L. Hedin, *Phys. Rev.* **139**, A796 (1965).
- <sup>17</sup>B. I. Lundquist, *Phys. Kondens. Mater.* **6**, 193 (1967).
- <sup>18</sup>See, e.g., E. M. Lifshitz and L. P. Pitaevskii, *Statistical Physics Part 2* (Pergamon, Oxford, 1986).
- <sup>19</sup>G. Bongiovanni (private communication).
- <sup>20</sup>In fact it was shown in Ref. 19 that the exchange term in which the electrons jump from one subband to the other gives a sizable contribution to the self-energy for the second subband. This term was neglected here and I believe that it does not have a strong influence on the shape of the intersubband absorption line.
- <sup>21</sup>M. Zachau, *Semicond. Sci. Technol.* **3**, 879 (1988).
- <sup>22</sup>M. Berz (private communication).